IL NUOVO CIMENTO **45 C** (2022) 75
DOI 10.1393/ncc/i2022-22075-x

COMMUNICATIONS: SIF Congress 2021

Robustness of a quasicrystalline higher-order topological insulator

SIMONE TRAVERSO(*)

Dipartimento di Fisica, Università degli Studi di Genova - Genova, Italy

received 28 January 2022

Summary. — It was recently discovered that quasicrystalline systems may provide a platform for the realisation of higher order topological insulators, where the topological phase is protected by spatial symmetries. In this paper I focus on a specific model and study the robustness of its topological phase against perturbations of the protecting symmetry. This is done both by varying the shape of the sample and by deforming the lattice. While signatures of the higher order topological phase can persist, the effects of an even slight symmetry breaking are significant.

1. – Introduction

The quest for new playgrounds for electronics, spintronics, and quantum computation led, around twenty years ago, to a remarkable change of paradigm in condensed matter physics [1-21]. The usual classification of crystalline materials in conductors and insulators has been surpassed with the discovery of topological insulators, a special class of materials in which an insulating bulk coexists with metallic states that live at the system's boundaries [1]. The edge states found in topological insulators are protected against elastic backscattering and this protection is often provided by a symmetry of the system (typically time-reversal [2,3]). Moreover, the topological phase, and consequently the associated edge states, will not disappear if the system parameters are modified by some perturbation, unless it is strong enough to cause gap closing [1].

In topological insulators, the metallic edge states are confined in one spatial dimension less than the hosting system. This link between a non-trivial topology of the d-dimensional bulk bands and the presence of boundary states of dimension $d-1$ is called *bulk-boundary correspondence*.

In recent years, it has been discovered that this correspondence might have exceptions. Different topological crystalline phases can occur in which the boundary states live in a dimension lower than $d-1$. Systems that manifest this particular signature are called *Higher Order Topological Insulators* (HOTI) [22, 23].

(*) E-mail: simone.traverso@edu.unige.it

Together with the development of HOTIs, a new material was recently synthesised: the twisted bilayer graphene [24]. When the rotation angle between the two sheets is set to thirty degrees, [25] the structure becomes a graphene-based quasicrystal (GQ), hence lacking discrete translational invariance. However, the material possesses long range order in the form of a 12-fold rotational symmetry (C_{12}). The GQ is of great interest in the field of HOTIs: indeed, being a quasicrystal, it presents rotational symmetries not achievable by crystalline materials and so it can give birth to a HOTI phase not observable in the latter [26, 27].

A remarkable GQ-based HOTI model is the one proposed by Stephen Spurrier and Nigel R. Cooper in [27]. This model realises a Second Order Topological Insulator (SOTI) phase, meaning that the bulk gap is two-dimensional while the topological modes are zero-dimensional (0D). The symmetry protecting the SOTI phase is the C_{12} rotational symmetry. While the bulk necessarily has this symmetry, in finite size samples the geometry of the boundary needs to be chosen carefully in order to have the C_{12} as a global symmetry and hence being sure to observe the HOTI phase. If this is done, the SOTI phase is characterised by the presence of in-gap degenerate eigenvalues associated to 0D states localised on the vertices of the sample (corner modes).

In this paper, taking the model proposed by S. Spurrier and N. Cooper as a platform, I study the robustness of the SOTI phase with respect to geometrical disorder. Through a numerical tight-binding approach, the effect of two kinds of geometrical perturbations will be analysed: the first one consists in a variation of the rotation angle between the two superimposed hexagonal lattices (and so amounts to a deformation of the full lattice); the second in choosing a sample shape not compatible with the C_{12} symmetry.

It will be shown that, in both cases, the rotational symmetry breaking causes a degeneracy lifting in the spectrum signature of the SOTI phase. Moreover, it will be demonstrated that the edges play a crucial role in the realisation of the SOTI phase.

The article is structured as follows. In sect. **2**, I will describe the SOTI model and the perturbations that will be subsequently inspected. In sect. **3**, the results are presented. In sect. **4**, the interpretation is given. Finally, in sect. **5**, a conclusive discussion is presented.

2. – Model

The HOTI model under inspection consists of two layers —t, b for top and bottom respectively— of graphene lattice. Such system is populated by spinless electrons, whose creation operators on the i-th lattice site of the layer t/b are $c_i^{\dagger,t/b}$. The fermions undergo in-plane nearest neighbours hopping with amplitude t, and next to nearest neighbour hopping with complex amplitude $i\nu_{ij}$ given by the usual Haldane coupling [28]. Moreover, a distance-dependent inter-layer hopping is present, parametrised by $t_{ij}^{\perp}$. More specifically, I set the interlayer coupling t_{ij} as exponentially decreasing with the distance between the sites on the two layers with the explicit form

$$t_{ij}^{\perp} = t^{\perp} \exp\left(-\frac{|\vec{d}_{ij}| - d_0}{\delta}\right), \tag{1}$$

where $\vec{d}_{ij}$ is the vector that connects the i and j sites on the two planes; $\delta = 0.184a$ is the decay length of the transfer integral (expressed in units of the in-plane next-nearest neighbour distance a); d_0 is the interlayer distance and $t^{\perp}$ is a coupling coefficient. The

two layers are twisted with respect to each other by a 30 degree angle. The tight-binding Hamiltonian then reads [27]

$$H = t \sum_{\langle ij \rangle} c_i^\dagger \tau_0 c_j + \lambda_H \sum_{\langle\langle ij \rangle\rangle} i\nu_{ij} c_i^\dagger \tau_z c_j + \lambda_\perp \sum_{ij} t_{ij}^\perp c_i^\dagger \tau_x c_j. \tag{2}$$

Here $\langle ij \rangle$ and $\langle\langle ij \rangle\rangle$ denote the pairs of intralayer nearest and next-nearest neighbour sites respectively, while the Pauli matrices τ_i act in the space of layer isospin, where the $c_i = (c_i^t, c_i^b)^T$ operator is defined. In other words, the Hamiltonian consists of two Haldane models [28] with opposite Chern number —which is nothing more than the Kane-Mele model [2] with the spin replaced by layer isospin— and with a 30 degrees twist coupled together by a term of interlayer hopping.

The results described throughout this article have been obtained by adopting a numerical tight-binding approach. The *pybinding* package has been used for the construction and diagonalisation of the system Hamiltonian [29]. Moreover, the following parameters have been adopted: $\lambda_H = 0.3t$([1]) and $t_\perp = -0.178t$. The $t_\perp$ coefficient is chosen so that if the auxiliary parameter $\lambda_\perp$ is set to one, then the interlayer coupling intensity matches what is experimentally observed for real TBG samples, as reported for example in [30]. The $\lambda_\perp$ coefficient is redundant, and is added only to have a means for tuning the interlayer interaction intensity in units of the real system coupling $t^\perp$: indeed, for limited sample sizes, it may be necessary for the gap to open (and so host the corner states) to increase $\lambda_\perp$ above the unity value. To avoid unnecessary computational complexity, the interlayer coupling has been limited to sites whose relative distance $|\vec{d}|$ satisfies $|\vec{d}| - d_0 < 2a_{cc}$, with a_{cc} the in-plane nearest neighbour distance. As a matter of fact, over this distance the interlayer coupling can be safely neglected. In what follows, the nearest neighbour distance is set as in graphene ($a_{cc} = 0.142\,\text{nm}$) and the system sizes are reported in SI units instead of units of this distance, for easier confrontation with experimentally achievable samples.

For $\lambda_\perp = 0$, and taking a finite sample, one finds counter-propagating metallic modes localised on the edges of the two planes —as in [2], but with spin replaced by layer isospin. The role of the interlayer hopping term is to gap out the counter-propagating metallic modes on the edges of the two planes. Surprisingly, under the appropriate conditions on the choice of the boundaries, zero energy modes localised at the corners survive, so that the HOTI phase can occur. This is indeed the case if the sample is dodecagonal and one of the edges is of the armchair type. For this case, the result is shown in fig. 1(a), where, more specifically, the low-energy spectrum obtained for a system with an apothem of 30.7452 nm is shown. As already reported in [27], it is found that the interlayer interaction gaps out the zero-energy counter propagating modes on the two planes and the gap hosts a group of twelve degenerate eigenvalues. These correspond to states localised on the vertices of the dodecagonal sample, as can be seen from the density plot in fig. 1(b); such 0D corner modes are a clear signature of the Second Order Topological phase realised by the model.

The target of this paper is to study the stability of the SOTI phase, just described, with respect to the presence of geometrical perturbations. As anticipated, this will be done both by varying the rotation angle between the two planes while keeping the

([1]) The Haldane term is not present in real TBG samples, so it can be set at any desired value as long as the $|\lambda_H| < 1/3$ condition is respected. See [28] for a complete discussion.

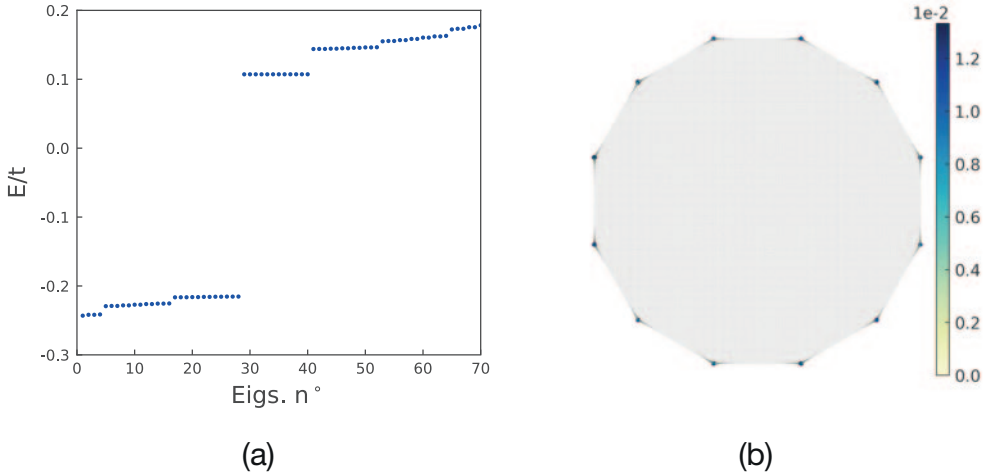

Fig. 1. – Panel (a): low-energy eigenvalues obtained by diagonalising Hamiltonian (2) for a dodecagonal sample with an apothem of 30.7452 nm, setting $\lambda_\perp = 2$; all the other parameters are set as specified in the main text. Panel (b): density plot of the square modulus of an eigenstate associated to one of the twelve degenerate in-gap eigenvalues on the left.

dodecagonal structure, and so applying a deformation to the lattice, and by taking a sample with a shape not compatible with the C_{12} symmetry.

As far as the first analysis is concerned, it is necessary to carefully explain what varying the rotation angle actually means: first of all, without loss of generality, I assume to keep the lower plane fixed and rotate the upper one. Then two possibilities appear. One can first rotate the upper layer of 30 degrees, then crop the bilayer with a dodecagonal shape and finally vary again the rotation angle: this way the two individual layers remain exactly as in the 30° configuration, but the overall sample will not be an exact dodecagon anymore; let us call this method 1. On the other hand, one can first rotate the upper layer of the desired angle (for example 29.9 degrees) and then crop the bilayer system into a dodecagonal sample: this way, for different rotation angles, the upper layer will present a different configuration of its sites (especially on the edges), but the system will always correctly fit the dodecagonal shape; let us call this method 2.

As for the second analysis, an octagonal shape will be considered. In fact, for an octagonal geometry, the shape symmetry is not compatible with the C_{12} bulk symmetry of GQ. Among other things, this causes some of the edges to be "badly shaped". I will return on this later on.

3. – Results

Here, the results obtained from the diagonalisation of the model in eq. (2) under the geometrical perturbations described above are presented.

3˙1. *Variation of the rotation angle.* – Before presenting the results obtained varying the angle of relative rotation between the two planes of the bilayer system —that from now on will be denoted as θ— both with method 1 and method 2, a clarification is needed: it must be noted that up to a variation that causes a modification of the upper

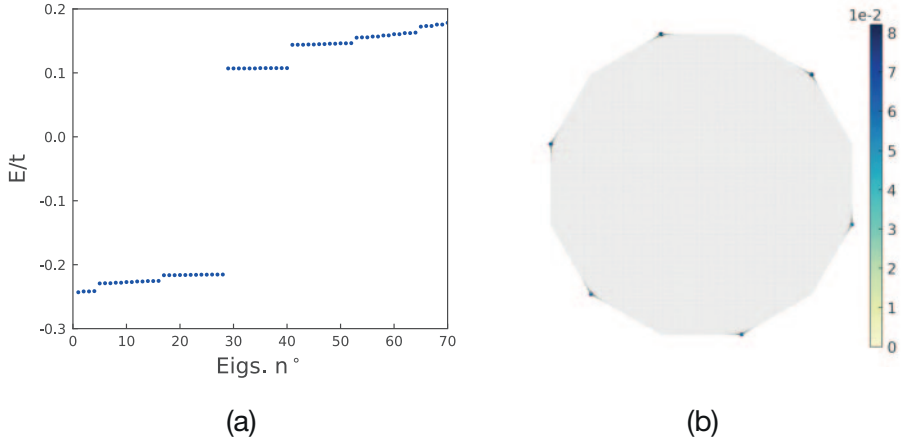

Fig. 2. – Panel (a): low-energy eigenvalues obtained by diagonalising Hamiltonian (2) for a dodecagonal sample with an apothem of 30.7452 nm, for $\theta = 29.995°$ and $\lambda_\perp = 2$; all the other parameters are set as specified in the main text. Panel (b): density plot of the square modulus of an eigenstate associated to one of the six degenerate eigenvalues in the higher-energy in-gap group on the left.

layer edge sites, there will be no differences between applying one method or the other([2]). A technical note: in the remainder of this subsection it is assumed that $\lambda_\perp = 2$ and the apothem of the dodecagonal sample is 30.7452 nm.

Let us start by considering an angle very close to 30°, for which the two methods bring the same result. In fig. 2(a), the low-energy eigenvalues obtained setting $\theta = 29.995°$ are presented. Except for the rotation angle, all the other parameters are taken as in fig. 1(a), for an easier comparison. At first sight it would seem that from fig. 1(a) to fig. 2(a) nothing changes and that there are still twelve degenerate eigenvalues inside the gap. Actually, by taking a closer look to the numerical value of the energy levels —omitted for brevity— one finds that the degeneracy is lifted: for $\theta = 29.995°$ the twelve in-gap modes separate in two groups of 6-fold degenerate eigenvalues. The eigenvalues of the two groups correspond to eigenstates with distinct localisation pattern: more precisely, the associated states are still corner modes, but each group is localised on six of the twelve corners, as can be seen from the density plot in fig. 2(b).

Now let us consider a bigger deviation from the 30°-twist (and so from the quasicrystalline phase). For $\theta = 29.95°$ method 1 and method 2 bring different results, as shown in fig. 3(a) and fig. 3(b). By comparing the first with fig. 2(a), it appears that the degeneracy lifting inside the group of twelve eigenvalues is now slightly more visible; the two groups of 6-fold degenerate eigenvalues inside the gap still correspond to states localised on alternate corners, as in fig. 2(b), but with longer localisation length (density plot not shown). Diagonalising for yet greater deviations from the thirty degrees, one would find

([2]) The value of $\delta\theta$ for which the sites of the upper edges change in order to fit the shape, depends on "how tight" the geometrical container is. This is mainly a computational problem: the finite size system is constructed by specifying a geometrical box, that can be taken more or less tight. The physically relevant aspect is to make clear what the "right way" of varying θ is in a finite size TBG system.

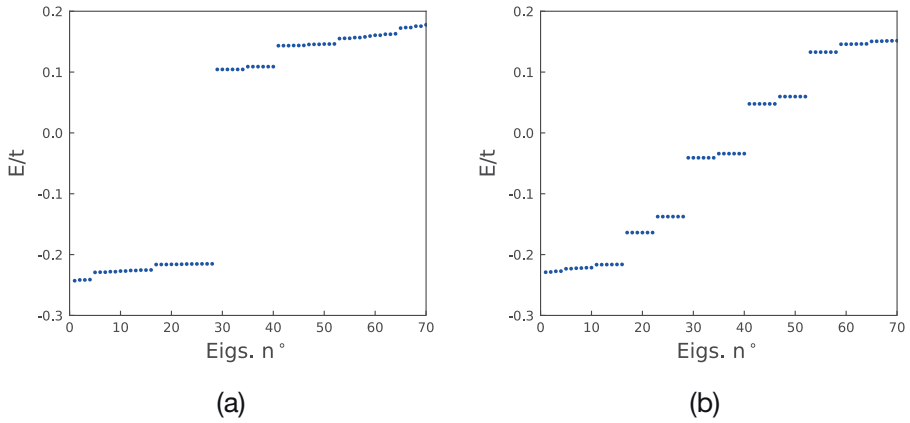

Fig. 3. – Panel (a): low-energy eigenvalues obtained by diagonalising Hamiltonian (2) for a dodecagonal sample with an apothem of 30.7452 nm; θ has been set to 29.95° while applying method 1, $\lambda_\perp = 2$ and all the other parameters are set as specified in the main text. Panel (b): low-energy eigenvalues obtained by diagonalising Hamiltonian (2) for a dodecagonal sample with an apothem of 30.7452 nm; θ has been set to 29.95° while applying method 2, $\lambda_\perp = 2$ and all the other parameters are set as specified in the main text.

that the splitting energy and the localisation length increase in a continuous way ([3]). On the other hand, things are quite different when following method 2: what happens here is that cropping with a dodecagonal shape for $\theta = 29.95°$ causes some sites on the edges of the upper layer to change with respect to the 30° configuration. This can be seen by directly inspecting the borders of the finite size lattice (not reported here). The modification of the sites on the edges turns out in the spectrum depicted in fig. 3(b), that is drastically different with respect to the ones in fig. 2(a) and fig. 3(a). Indeed, it presents a proliferation of groups of 6-fold degenerate eigenvalues inside the gap, which no longer correspond to 0D corner modes (density plots not shown). The application of method 2 for bigger variations of the rotation angle causes further changes of the edges and, as a consequence, in the low energy spectrum, that rapidly comes to bear no resemblance with the initial one.

3˙2. *Octagonal shape*. – Here, the effect induced on the topological phase by picking up a polygonal shape not compatible with the bulk symmetry is analysed. In fig. 4(a), the results obtained from the diagonalisation of Hamiltonian (2) for a sample with octagonal shape are shown. The diagonalisation has been performed taking $\lambda_\perp = 1$ and considering a sample with an apothem of 22.0139 nm.

Observing the low energy spectrum in fig. 4(a), one sees that it presents striking differences with respect to the one obtained for the dodecagonal sample. The interlayer interaction still opens a gap, but this time the gap hosts many groups of four-times degenerate eigenvalues. In fig. 4(b), the density plot for one of these states is reported: one finds that its wave function, instead of being localised on the vertices like in the

([3]) At least up to the point where the mismatch of the two edges of the two layers is too pronounced for them to be gapped out by the interlayer interaction. The value of $\delta\theta$ for which this happens depends from the sample size.

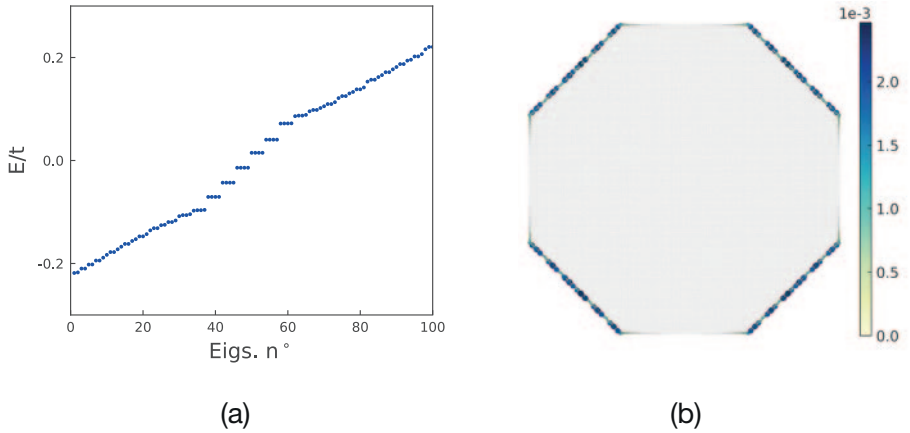

Fig. 4. – Panel (a): low-energy eigenvalues obtained by diagonalising Hamiltonian (2) for an octagonal sample with an apothem of 22.0139 nm, setting $\lambda_\perp = 1$; all the other parameters are set as specified in the main text. Panel (b): density plot of the square modulus of an eigenstate associated to an eigenvalue that belongs to the degenerate in-gap quadruplets on the left.

dodecagonal case, is delocalised on four of the eight edges of the octagon while it vanishes on the other four. Actually, the four edges where the probability density doesn't go to zero are just those that are not compatible with the C_{12} symmetry of the quasicrystal bulk.

Increasing the sample size, the conclusions remain qualitatively the same: one still finds groups of 4-fold degenerate eigenvalues, which correspond to states localised on the four edges not compatible with the C_{12} symmetry (not shown). The only difference is that the number of these quadruplets of degenerate eigenvalues proliferates with the sample size. This feature is most likely due to the quasicrystalline nature of the structure considered which implies that all length scales actually matter.

4. – Discussion

In sect. **3**˙1 I showed that even a minimal deformation of the lattice ($\theta = 29.995°$) breaks the topological phase as described in [27], lifting the degeneracy between the twelve in-gap eigenvalues and modifying the localisation pattern of the associated corner modes. That said, the perturbed system has some interesting features too: the twelve degenerate eigenvalues split in two 6-fold degenerate eigenvalues that correspond to 0D modes localised on alternate corners of the sample. Most likely, this happens because when the two layers are slightly mismatched, the system has C_6 symmetry: indeed, if one rotates each individual layer of 60°, the geometrical distribution of the sites remains unchanged.

On the other hand, the topological signature is completely altered when the sites on the edges undergo a modification. A proof of this is given by the low energy spectrum reported in fig. 3(b), which was obtained by varying the bilayer rotation angle while adopting method 2.

The role of the edges in the realisation of the higher order topological phase becomes even more obvious in the light of the results reported in sect. **3**˙2. There, it was shown that considering an octagonal sample, the probability density of the in-gap 4-fold degen-

erate([4]) states goes to zero on four of the eight edges, while it is equally distributed on the other four (fig. 4(b)). As already mentioned, the four edges on which the probability density vanishes are those that are compatible with the lattice bulk symmetry([5]).

The reason for which on the octagonal sample the in-gap states are localised only on the "badly cropped" edges —those not compatible with the bulk symmetry– is that their border sites present bad superposition between the two layers. In sect. **2** it was explained that the interlayer coupling is responsible for gapping out the counter propagating Haldane modes on the edges of the two planes: however, because of its trend of decreasing exponential, this mechanism of gap opening only works if the border sites on the upper and lower layer perfectly overlap. This condition is met on the four edges compatible with the C_{12} symmetry, but not on the "badly cropped" four ones.

This analysis proves that, at least for this model, in order to have 0D localised states on the vertices of a polygonal sample it is necessary that *all* the edges are cropped in a way that is compatible with the bulk C_{12} symmetry, which, in the end, is the symmetry protecting the SOTI phase described in [27].

5. – Conclusions

By considering a specific model for a C_{12}-protected SOTI on a quasicrystal, I have shown that this kind of topological phase is extremely fragile against geometrical perturbations. Moreover, I have proven that in order to achieve a higher order topological phase, at least for the model considered, the compatibility of the sample edges with the bulk protecting symmetry plays a crucial role. In addition, I have found that the analysed model, due to its quasicrystalline nature, presents an incredibly rich phenomenology that certainly deserves further study.

* * *

I thank Niccolò Traverso Ziani and Maura Sassetti for their continued help; I also thank Stephen Spurrier for useful discussion. This work was supported by the "Dipartimento di Eccellenza MIUR 2018-2022".

REFERENCES

[1] Hasan M. Z. and Kane C. L., *Rev. Mod. Phys.*, **82** (2010) 3045.
[2] Kane C. L. and Mele E. J., *Phys. Rev. Lett.*, **95** (2005) 226801.
[3] Kane C. L. and Mele E. J., *Phys. Rev. Lett.*, **95** (2005) 146802.
[4] Bernevig B. A., Hughes T. L. and Zhang S.-C., *Science*, **314** (2006) 1757.
[5] König M., Weidmann S., Brüne C., Roth A., Buhmann H., Molenkamp L. W., Qi X.-L. and Zhang S.-C., *Science*, **318** (2007) 766.
[6] Qi X.-L., Hughes T. L. and Zhang S.-C., *Nat. Phys.*, **4** (2008) 273.
[7] Fu L. and Kane C. L., *Phys. Rev. B*, **79** (2009) 161408(R).
[8] Knez I., Du R.-R. and Sullivan G., *Phys. Rev. Lett.*, **107** (2011) 136603.
[9] Väyrynen J. I. and Ojanen T., *Phys. Rev. Lett.*, **107** (2011) 166804.
[10] Dolcetto G., Sassetti M. and Schmidt T. L., *Riv. Nuovo Cimento*, **39** (2016) 113.

([4]) Again, the fact that the in-gap eigenvalues are clustered in groups with a degeneracy of four, is most likely due to the fact that the octagonal sample has a global C_4 symmetry.
([5]) Note that for a lattice with the symmetries of GQ cropped in an octagonal shape there can be four edges compatible with the lattice symmetry —and so "well cropped'— at most.

[11] Dolcetto G., Traverso Ziani N., Biggio M., Cavaliere F. and Sassetti M., *Phys. Status Solidi (RRL)*, **7** (2013) 1059.
[12] Dolcetto G., Traverso Ziani N., Biggio M., Cavaliere F. and Sassetti M., *Phys. Rev. B*, **87** (2013) 235423.
[13] Hart S., Ren H., Wagner T., Leubner P., Mühlbauer M., Brüne C. and Buhmann H., *Nat. Phys.*, **10** (2014) 638.
[14] Li J., Pan W., Bernevig B. A. and Lutchyn R. M., *Phys. Rev. Lett.*, **117** (2016) 046804.
[15] Reis F. *et al.*, *Science*, **357** (2017) 287.
[16] Traverso Ziani N., Fleckenstein C., Dolcetto G. and Trauzettel B., *Phys. Rev. B*, **95** (2017) 205418.
[17] Wu S. *et al.*, *Science*, **359** (2018) 76.
[18] Fleckenstein C., Traverso Ziani N. and Trauzettel B., *Phys. Rev. Lett.*, **122** (2019) 066801.
[19] Traverso Ziani N., Fleckenstein C., Vigliotti L., Trauzettel B. and Sassetti M., *Phys. Rev. B*, **101** (2020) 195303.
[20] Fleckenstein C., Traverso Ziani N., Calzona A., Sassetti M. and Trauzettel B., *Phys. Rev. B*, **103** (2021) 125303.
[21] Strunz J. *et al.*, *Nat. Phys.*, **16** (2020) 83.
[22] Schindler F., Cook A. M., Vergniory M. G., Wang Z., Parkin S. S. P., Bernevig B. A. and Neupert T., *Sci. Adv.*, **4** (2018) eaat0346.
[23] Trifunovic L. and Brouwer P. W., *Phys. Status Solidi B*, **258** (2021) 2000090.
[24] Cao Y. *et al.*, *Nature*, **556** (2018) 43.
[25] Ahn S. J., Moon P., Kim T.-H., Kim H.-W., Shin H.-C., Kim E. H., Cha H. W., Kahng S.-J., Kim P., Koshino M., Son Y.-W., Yang C.-W. and Ahn J. R., *Science*, **361** (2018) aar8412.
[26] Chen R., Chen C.-Z., Gao J.-H., Zhou B. and Xu D.-H., *Phys. Rev. Lett.*, **124** (2020) 036803.
[27] Spurrier S. and Cooper N. R., *Phys. Rev. Res.*, **2** (2020) 033071.
[28] Haldane F. D. M., *Phys. Rev. Lett.*, **61** (1988) 2015.
[29] Moldovan D., Andelković M. and Peeters F., *pybinding v0.9.5: a Python package for tight-binding calculations (v0.9.5)*, Zenodo (2020) `https://doi.org/10.5281/zenodo.4010216`.
[30] Moon P. and Koshino M., *Phys. Rev. B*, **85** (2012) 195458.